Rheological and Structural Investigation of Layered Silicate Nanocomposites Based on Polyamide or Polyethylene: Influence of Processing Conditions and Volume Fraction Effects

Pascal Médéric,*[1] *Tolotrahasina Razafinimaro*,[1] *Thierry Aubry*,[1] *Michel Moan*,[1] *Marie-Hélène Klopffer*[2]

[1] Laboratoire de Rhéologie, Université de Bretagne Occidentale, 6, avenue Victor Le Gorgeu, C.S. 93837, 29238 Brest cedex 3, France
Fax: 33 (0)2 98 01 79 30; E-mail: pascal.mederic@univ-brest.fr
[2] Institut Français du Pétrole, B.P. 311, 1-4 avenue Bois-Préau, 92506 Rueil-Malmaison, France

Summary: Organoclay polymer nanocomposites offer improved material properties at very low filler loadings making them of immediate interest for industrial applications. In this study two matrices are used : a polar polymer, PA12, and a non polar polymer, LLDPE. Many articles focused on the importance of the chemistry used to modify the surface of the clay. Numerous papers studied the influence of the compatibilizing agent necessary to obtain intercalated structure, when the matrix is non polar. This paper demonstrates the importance of the way the clay was melt processed into the thermoplastic matrix. Layered silicate nanocomposites based on PA12 or LLDPE were characterized by X-ray diffraction, transmission electron microscopy and rheological tests. The influence of volume fraction on rheological and structural properties is also investigated.

Keywords: layered silicates; nanocomposites; polyamide; polyethylene; processing conditions; rheology

Introduction

Polymer/layered silicate nanocomposites have become an important class of polymeric composites because they exhibit dramatic enhancements in barrier,[1,2] thermal[3,4] and mechanical[5,6] properties even at very low silicate contents. It is generally acknowledged that these properties are strongly affected by the affinity between matrix and clay,[7] the degree of clay exfoliation, the degree of dispersion and the orientation of clay particles throughout the thermoplastic matrix.[8] The chemical strategy used to modify the surface of the clay and the

 DOI: 10.1002/masy.200550308

melt processing conditions play a key role in achieving the structure and properties of the final product.[9] So the study of the rheological behavior of these systems, correlated with other investigation techniques, such as Electron Microscopy and X-Ray Diffraction, is of great importance.[10-12] This work focuses on the influence of the melt-blending conditions and the particle volume fraction on the structure and melt rheological properties of polymer/layered silicate nanocomposites.

Experimental

The first system was prepared from a commercial polymer, a polyamide 12 (Rilsan® AECHVO from Atofina) and a commercial modified montmorillonite clay, referenced as C30B, supplied by Southern Clay Products (Gonzales, TX). The melting point of this PA12 grade is 178°C. Using thermogravimetric analysis, the weight loss of the polyamide 12 used in this work was shown to be less than 0.5% after 45min at 220°C.[13] Its weight and number average molecular weights were shown to be 37 000g/mol and 20 000g/mol respectively.[13] C30B is a methyl bis-2-hydroxyethyl tallow exchanged montmorillonite clay with a modifier concentration of 90 meq/100g. This treatment is adjusted to ascertain a good dispersion in the polar PA matrix and to make a nanocomposite of intercaled or exfoliated type. Indeed, the hydroxyl groups of the organic modifier are able to interact with amine groups of PA via numerous hydrogen bonds.

The second system was made from a commercial linear low density polyethylene (LLDPE, Flerixene FG20F from Enichem) and a commercial modified montmorillonite clay, referenced as C20A, supplied by Southern Clay Products (Gonzales, TX). This PE grade was already used in previous rheological studies.[14,15] Its melting point is 121°C and its weight and number average molecular weights are 140000g/mol and 37000g/mol respectively. C20A is a dimethyl dihydrogenated tallow ammonium montmorillonite clay with a modifier concentration of 95 meq/100g. Due to the low polarity of the alkyl chains, intercalation of polyolefin macromolecules requires the addition of a compatibilizing agent. Anhydride maleic has already been proved to have a high intercalation level with the clay layers.[16-19] This compatibilizer, denoted C, is a maleic anhydride grafted-PE, provided by Atofina. Its melting point is 124°C and its weight and number average molecular weights are 92500g/mol and 20000g/mol respectively.

Both organoclays (C30B and C20A) are thermally stable at the temperatures of this study.[5,20] Composites have been prepared at solid volume fractions Φ ranging from 0% to 12%, by using an internal mixer. Oscillatory and steady shear measurements were performed using a Rheometrics Dynamic Analyser (RDAII) equipped with parallel disks of 25mm diameter and 2mm spacing. Rheological measurements were performed under a nitrogen blanket and carried out at a temperature of 200°C for PA12-based composites, and 195°C for PE-based composites. Data on dynamic moduli and complex vicosity correspond to the higher strain amplitude (4%) for which the response of all systems is linear viscoelastic. PA12 and C30B/PA12 nanocomposites were dried for 4h at 85°C under vacuum before experiments. The structure and morphology of these filled systems were observed by using Wide-Angle X-Ray Scattering, Scanning Electron Microscopy and Transmission Electron Microscopy techniques. X-Ray diffraction patterns were obtained using a Siemens F X-ray diffractometer with Ni-filtered Cu Kα radiation of wavelength 0.15nm, generated at 35kV and 25mA. Data were recorded in the range of $2\theta = 2\text{-}5°$ using a counting time and a step size of 8s and 0.02° respectively. For Transmission Electron Microscopy observations, ultrathin sections were prepared at –100°C with an Ultracut E ultracryomicrotome (Reichert and Jung) using a diamond knife. Imaging was performed with a Zeiss EM 902 at 80kV. The morphology of C20A/PE system (system without compatibilizer) was observed, using a Scanning Electron Microscopy on cryo-fractured surfaces.

Results and Discussion

A. C30B/PA12 nanocomposites

In the first part of this work, the effect of processing conditions (and more particularly the rotational speed of the blades during mixing) on the formation of C30B/PA12 nanocomposites is studied. Three 2.5% C30B/PA12 composite samples, denoted S_1, S_2 and S_3, have been prepared with a mixing time of 6 minutes, that is the time needed to obtain a constant torque on the blades, at different rotational speeds, respectively 32rpm, 65rpm and 100rpm. Figure 1 shows the diffraction patterns from the organically modified clay, C30B, and the systems S_1, S_2 and S_3. The d_{001} basal reflection peak of C30B appears at $2\theta = 4.5°$, corresponding to an interlayer gallery of 1nm. For S_1, this peak is shifted to $2\theta = 2.7°$, i.e. a d-

spacing of 2.3nm, suggesting a partial intercalated structure. Indeed PA12 chains diffuse into the host silicate layer galleries, due to the numerous weak interactions between PA12 and modified clay surfaces, thereby producing an expanded polymer-silicate layer structure. The disappearance of this peak, or the reduction in its intensity indicates a partially exfoliated structure for S_2 and S_3.[21] Increasing rotational speed finally leads to exfoliation : platelets move away from each other via shear-induced diffusion of PA12 chains in the organoclay gallery.[22]

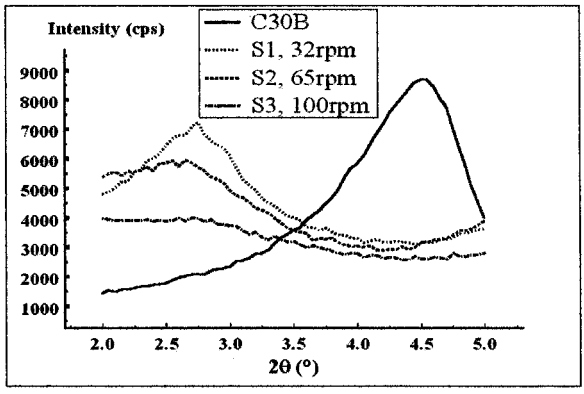

Figure 1. Rotational speed dependence of X-ray diffraction patterns for S_1, S_2 and S_3.

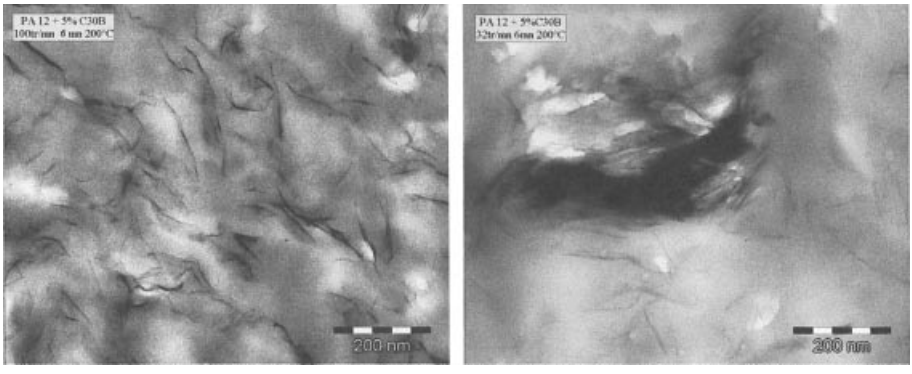

Figure 2. TEM micrographs : a) S_3 system (left), b) S_1 system (right).

Figure 2a shows a TEM micrograph of S_3 system. Exfoliated silicate layers are in a large majority. On the other hand, Figure 2b shows the structure of the S_1 system. In fact, the presence of few exfoliated silicate layers and silicate anisotropic stacks (characteristic size ~500nm) is evidenced in Figure 2b. These observations are in accordance with diffraction spectra of nanocompsite samples.

Figure 3 shows the storage modulus G' versus circular frequency ω, for S_1, S_2 and S_3. S_2 and S_3 nanocomposites display a partial exfoliated nanostructure which leads to both a plateau-like behavior at low frequencies and enhanced viscoelastic moduli (G'' is not presented here) at high frequencies.[19] In addition, the storage modulus increases with increasing rotational speed, especially at the lowest frequencies. The storage modulus level for S_1 is three times lower than that of S_3 in the terminal zone. This result shows that melt processing conditions play a key role in achieving high levels of exfoliation and dispersion. On the other hand the storage modulus values are very similar for S_2 and S_3.

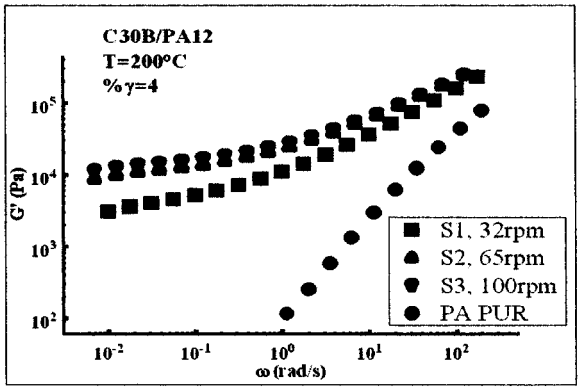

Figure 3. Rotational speed dependence of storage modulus for S_1, S_2 and S_3.

In the second part of this work, the influence of volume fraction on rheological properties of C30B/PA12 nanocomposites is studied. The low frequency relative complex viscosity versus clay volume fraction plot is displayed in Figure 4. Considering the low C30B volume fractions ($\Phi < 0.75\%$), the method described by Utracki[23] is used and yields a C30B aspect

ratio equal to 140 for the system processed at 32 rpm and 330 for the system processed at 100 rpm. For the last system, assuming a layer thickness of 1nm, the diameter of an isolated clay particle is thus calculated to be 330nm. This result is in very good agreement with average sizes of montmorillonite exfoliated layers.[24] On the other hand, the inferior aspect ratio calculated for the system mixed at 32rpm is indicative of the presence of stacks. These conclusions confirm the XRD and TEM observations for the systems S_3 and S_1.

All results show that optimized processing conditions are a mixing time of 6mn and a rotational speed of 100rpm. Thus, these conditions are used in the following part of this study.

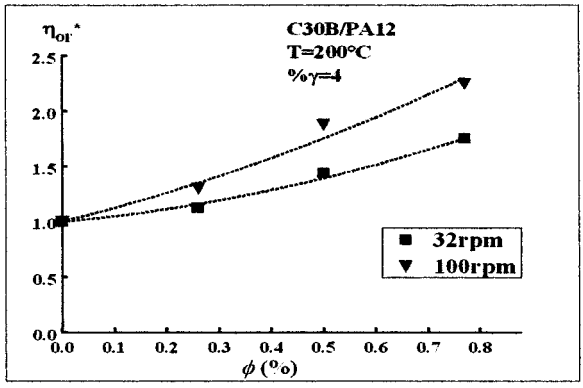

Figure 4. Clay volume fraction dependence of low frequency relative complex viscosity for C30B/PA12.

Figure 5 shows the storage modulus as a function of frequency, in the linear viscoelastic domain for different volume fractions. Although the qualitative behavior of the storage and loss moduli (only G' is presented in Figure 5) are essentially unaffected by increasing clay content in the high frequency range, at low frequencies the viscoelastic behavior changes from liquid-like to solid-like behavior.[25] For sufficiently filled nanocomposites, platelet-platelet interactions are mainly responsible for this change which affects more strongly the storage than the loss modulus. The large enhancement of elastic modulus G' at low frequencies and the frequency independence of the loss tangent G''/G'[25] appear at a critical volume fraction of about 1% and mark the liquid-solid transition. This critical volume fraction is also highlighted in Figure 6 which shows the variation of the first normal stress coefficient

ψ_1 versus shear stress τ. In fact, for volume fractions lower than 1%, a low shear plateau is observed. It is not the case for sufficiently filled systems ($\Phi \geq 1\%$).

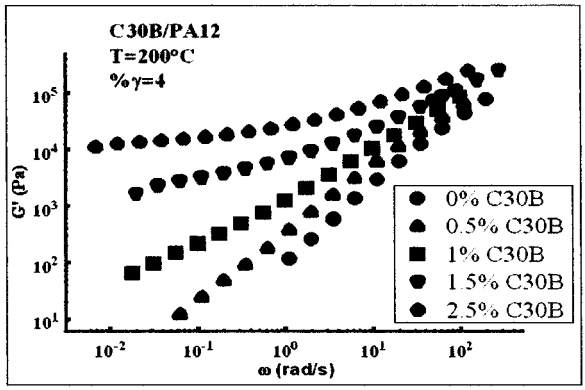

Figure 5. Clay volume fraction dependence of storage modulus for C30B/PA12.

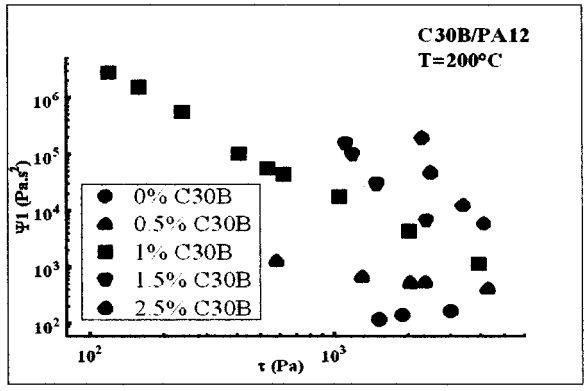

Figure 6. Clay volume fraction dependence of first normal stress coefficient for C30B/PA12.

B. C20A/C/LLDPE Nanocomposite

Because LLDPE does not include any polar group in its backbone, it does not form a nanocomposite structure by simple melt mixing of the organoclay (C20A) and the polymer.

Morphological investigation of C20A/LLDPE systems, as observed by Scanning Electron Microscopy (Figure 7), shows microaggregates formed by primary particles (~ 3μm).

A low frequency response indicative of a solid-like behavior is observed in the G' curve but only for a volume fraction of 12% (Figure 9). Such results are also obtained for conventional composites, such as talc/LLDPE.[26]

2.5%C20A/13%C/LLDPE system was studied. A two-step mixing sequence was used to prepare this system : organoclay/C master batch was prepared by melt mixing first, and then it was melt mixed with LLDPE.

Figure 8 shows the diffraction patterns from the organically modified clay, C20A, and the 2.5%C20A/13%C/LLDPE system. The d_{001} basal reflection peak of C20A appears at 2θ = 3.5°, corresponding to an interlayer gallery of 1.5nm. For 2.5%C20A/13%C/LLDPE system, this peak disappears. This is the signature of an exfoliated structure.

In Figure 9, this nanocomposite shows higher storage modulus over the whole frequency range than the 2.5%C20A/LLDPE. This rheological behavior is in agreement with XRD results. Additional studies are but needed to understand the relation between the structure and the melt rheological properties of C20A/C/LLDPE nanocomposites.

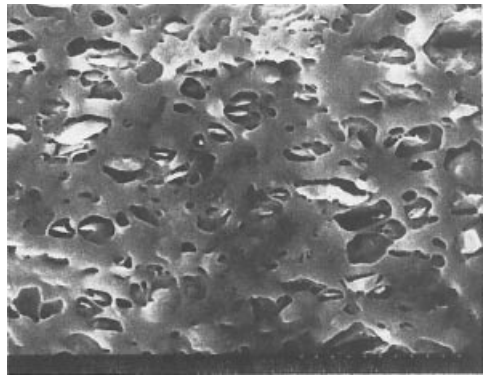

Figure 7. SEM micrographs for 2.5% C20A/LLDPE.

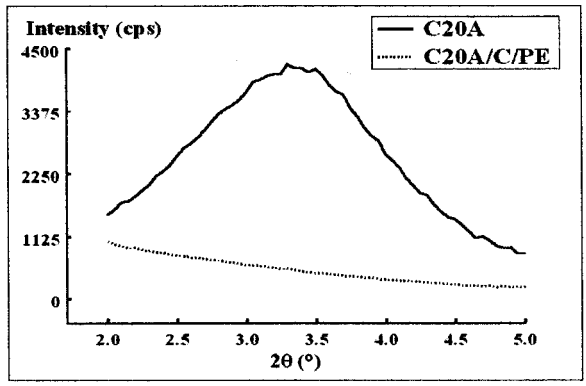

Figure 8. X-ray diffraction patterns for C20A clay and 2.5%C20A/13%C/LLDPE system.

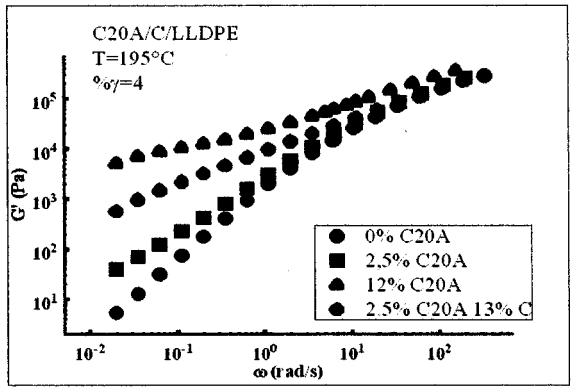

Figure 9. Frequency dependence of storage modulus for C20A/C/LLDPE.

Conclusions

It has been shown that the melt processing conditions have an important influence on the degree of delamination and dispersion of the platelets, thus on the microstructure and properties of the nanocomposite. The relation between the rheological behavior and the structure of C30B/PA12 was discussed : exfoliated structure is revealed not only through a

plateau-like G' behavior at low frequency but also enhanced viscoelastic moduli at high frequencies. The influence of the organoclay volume fraction on rheological behavior was studied. Preliminary rheological results concerning C20A/C/LLDPE systems were also presented.

Acknowledgments

The authors express thanks to Dr. F. Michaud, Université de Bretagne Occidentale, and Dr. Y. Fouquet, Ifremer, for XRD tests and Dr. B. Pees, Atofina, for TEM experiments.

[1] M. Krook, A.-C. Albertsson, U. W. Gedde, M. S. Hedenqvist, *Polymer Eng. & Sci.*, **2004**, *42(6)*, 1238.
[2] R. Waché, M.-H. Klopffer, S. Gonzales, P. Médéric, M. Moan, Eurofillers, Alicante, Spain, **2003**, 101.
[3] Y. Tang, Y. Hu, S. Wang, Z. Gui, Z. Chen, W. Fan, *Polymer international.*, **2003**, *52(8)*, 1396.
[4] Y. Tang, Y. Hu, S. Wang, Z. Gui, Z. Chen, *Polymers for adv. Technol.*, **2003**, *14(10)*, 733.
[5] J. W. Cho, D. R. Paul, *Polymer*, **2001**, *42(3)*, 1083.
[6] P. Reichert, J. Kressler, R. Thoann, R. Mülhaupt, G. Stöppelmann, *Acta Polym.*, **1998**, 49, 116.
[7] R. A. Vaia, E. P. Giannelis, *Macromolecules*, **1997**, *30*, 8000.
[8] H. R. Dennis, D. L. Hunter, D. Chang, S. Kim, J. L. White, J. W. Cho, D. R. Paul, *Polymer*, **2001**, *42*, 9513.
[9] S. S. Ray, M. Okamoto, *Prog. Polym. Sci.*, **2003**, *28*, 1539.
[10] J. Ren, A.S. Silva, R. Krishnamoorti, *Macromol.*, **2000**, *33*, 3739.
[11] R. Krishnamoorti, E. p. Giannelis, *Macromol.*, **1997**, *30*, 4097.
[12] D. F. Eckel, M. P. Balogh, P. D. Fasulo, W. R. Rodgers, *J. Applied Polym. Sci.*, **2004**, *93*, 1110.
[13] O. Talon, PhD thesis, INSA Rouen, France, **2002**.
[14] J. Huitric, P. Médéric, M. Moan, J. Jarrin, *Polymer*, **1998**, *39(20)*, 4849.
[15] M. Moan, J. Huitric, P. Médéric, J. Jarrin, *Journal of rheology*, **2000**, *44(6)*, 1227.
[16] A. Usuki, M. Kato, A. Okada, T. Kurauchi, *J. Applied Polym. Sci.*, **1997**, *63*, 137.
[17] M. Kawasumi, N. Hasegawa, M. Kato, A. Okada, A. Usuki, *Macromol.*, **1997**, *30(20)*, 6333.
[18] K. H. Wang, M. H. Choi, C. S. Koo, Y. S. Choi, I. J. Chung, *Polymer*, **2001**, *42*, 9819.
[19] Y. T. Lim, O. O. Park, *Rheologica Acta*, **2001**, *40*, 220.
[20] W. Xie, Z. Gao, K. Liu, W.-P. Pan, R. Vaia, D. Hunter, A. Singh, *Thermochimica Acta*, **2001**, *367/368*, 339.
[21] H. Ishida, S. Campbell, J. Blackwell, *Chem. Mater.*, **2000**, *12*, 1260.
[22] T.D. Fornes, P. J. Yoon, H. Keskkula, D.R. Paul, *Polymer*, **2001**, *42*, 9929.
[23] L. A. Utracki, J. Lyngaae-Jorgensen, *Rheol. Acta*, **2002**, *41*, 394.
[24] G. Lagaly, S. Ziesmer, *Adv. Colloid Interface Sci.*, **2003**,*100/102*, 105.
[25] H. H. Winter, M. M. Mours, *Adv. Polym. Sci.*, **1997**, *134*, 165.
[26] P. Médéric, M. Moan, M.-H. Klopffer, Y. Saint-Gérard, *Applied Rheology*, **2003**, *13(6)*, 297.